Goldstein, I. J., & Hayes, C. E. (1978) *Adv. Carbohydr. Chem. Biochem. 35*, 127–340.
Goodwin, G. C., Hammond, K., Lyle, I. G., & Jones, M. N. (1982) *Biochim. Biophys. Acta 689*, 80–88.
Grant, C. W. M., & Peters, M. W. (1984) *Biochim. Biophys. Acta 779*, 403–422.
Hampton, R. Y., Holz, R. W., & Goldstein, I. J. (1980) *J. Biol. Chem. 255*, 6766–6771.
Hoekstra, D. (1982a) *Biochemistry 21*, 2833–2840.
Hoekstra, D. (1982b) *Biochemistry 21*, 1055–1061.
Hoekstra, D. (1982c) *Biochim. Biophys. Acta 692*, 171–175.
Hoekstra, D., Düzgüneş, N., & Wilschut, J. (1985a) *Biochemistry 24*, 565–572.
Hoekstra, D., Wilschut, J., & Scherphof, G. (1985b) *Eur. J. Biochem. 146*, 131–140.
Kabat, E. A. (1978) *J. Supramol. Struct. 8*, 79–88.
Kelly, R. B., Deutsch, J. W., Carlson, S. S., & Wagner, J. A. (1979) *Annu. Rev. Neurosci. 2*, 399–446.
Maggio, B., Cumar, F. A., & Caputto, R. (1981) *Biochim. Biophys. Acta 650*, 69–87.
Nicolson, G. L., Blaustein, J., & Etzler, M. E. (1974) *Biochemistry 13*, 196–204.
Olden, K., Parent, J. B., & White, S. L. (1982) *Biochim. Biophys. Acta 650*, 209–232.
Papahadjopoulos, D. (1978) *Cell Surf. Rev. 5*, 765–790.
Rauvala, H. (1983) *Trends Biochem. Sci. (Pers. Ed.) 8*, 323–325.
Rendi, R., Vatter, A. E., & Gordon, J. A. (1979) *Biochim. Biophys. Acta 550*, 318–327.
Schuber, F., Hong, K., Düzgüneş, N., & Papahadjoulos, D. (1983) *Biochemistry 22*, 6134–6140.
Shechter, Y., Chang, K., Jacobs, S., & Cuatrecasas, P. (1979) *Proc. Natl. Acad. Sci. U.S.A. 76*, 2720–2724.
Slama, J. S., & Rando, R. R. (1980) *Biochemistry 19*, 4595–4600.
Sundler, R. (1982) *FEBS Lett. 141*, 11–13.
Sundler, R., & Wijkander, J. (1983) *Biochim. Biophys. Acta 730*, 391–394.
Surolia, A., Bachhawat, B. K., & Podder, S. K. (1975) *Nature (London) 257*, 802–804.
Utsumi, H., Suzuki, T., Inoue, K., & Nojima, S. (1984) *J. Biochem. (Tokyo) 96*, 97–105.
White, J., Kielian, M., & Helenius, A. (1983) *Q. Rev. Biophys. 16*, 151–195.
Wilschut, J., & Hoekstra, D. (1984) *Trends Biochem. Sci. (Pers. Ed.) 9*, 479–483.
Wilschut, J., Düzgüneş, N., Fraley, R., & Papahadjopoulos, D. (1980) *Biochemistry 19*, 6011–6021.

# X-ray Diffraction Evidence for Fully Interdigitated Bilayers of 1-Stearoyllysophosphatidylcholine†

S. W. Hui*
*Biophysics Department, Roswell Park Memorial Institute, Buffalo, New York 14263*
Ching-hsien Huang*
*Department of Biochemistry, University of Virginia School of Medicine, Charlottesville, Virginia 22908*
*Received July 17, 1985*

ABSTRACT: X-ray diffraction experiments have been performed on 1-stearoyllysophosphatidylcholine or C(18):C(0)PC as a function of hydration at temperatures below the order/disorder transition ($T_m$ = 26.2 °C). At these temperatures, hydrated C(18):C(0)PC forms lamellae. The bilayer thickness, as determined by the saturation hydration method and electron-density profile, is 35–36 Å, and the average area per C(18):C(0)PC molecule at the lipid/water interface is 45.5 Å$^2$. The packing geometry of C(18):C(0)PC in the lamella is proposed to adopt a fully interdigitated model in which the long C(18) acyl chain extends across the entire hydrocarbon width of the bilayer. Thus far, three different types of interdigitated bilayers are known for phosphatidylcholines. These various types of chain interdigitation are discussed in terms of the chain length difference between the *sn*-1 and *sn*-2 acyl chains.

It is generally recognized that in biological membranes most phospholipids self-assemble into two-dimensional arrays of the noninterdigitated lamellar type; that is, each phospholipid molecule is oriented with its polar head group toward the membrane surface and its chain methyl groups toward the geometric center of the hydrophobic core in the membrane interior. Recently, several spectroscopic studies have been directed to the investigation of aqueous dispersions of mixed-chain phospholipids including sphingomyelin, whose two hydrocarbons chains are inequivalent in terms of carbon number (Huang et al., 1984; Hui et al., 1984; Levin et al., 1985; McIntosh et al., 1984). Results of these studies indicate that in the gel state the packing mode of pure mixed-chain phospholipids in the two-dimensional array of lamellae is that of a highly ordered interdigitated bilayer, which is a marked deviation from the generally recognized noninterdigitated bilayer form of symmetric phospholipids. It is now established that at temperatures below the main order/disorder phase transition, mixed-chain phospholipid molecules can be accommodated in at least three different types of interdigitated packing modes, depending on the chain-length difference

† Supported, in part, by National Institutes of Health Grants GM-28120 and GM-17452.

0006-2960/86/0425-1330$01.50/0 

between the two hydrocarbon chains; they are designated as the partially interdigitated, mixed interdigitated, and fully interdigitated lamellae (Huang et al., 1984; Hui et al., 1984; Levin et al., 1985). Among the various detected packing modes, the fully interdigitated bilayer is a commonly observed model. The crystalline and gel phases of C(18):C(2)PC[1] serve as an example of this model, in which the longer hydrocarbon chain in a nearly all-trans conformation spans the entire hydrocarbon width of the bilayer (Huang et al., 1984). Consequently, the terminal methyl group of the longer chain is intercalated into the bilayer interface, and it is located in the vicinity of the carbonyl carbon in the opposing lamellar leaflet. It should be pointed out that the packing model of fully interdigitated bilayers has been proposed not only for mixed-chain phospholipids but also for symmetric phospholipids, whose acyl chains are saturated and of identical carbon numbers, under a wide range of experimental conditions (McDaniel et al., 1983; McIntosh et al., 1983; Ranck et al., 1977; Ranck & Tocanne, 1982a,b; Ruocco et al., 1985; Simon & McIntosh, 1984; Theretz et al., 1983).

Lysophosphatidylcholine is a molecular species of lipid that commonly occurs, albeit in minor amounts, in the mammalian cell membrane and the various membranes of subcellular organelles (Colbeau et al., 1976; Nelson, 1967). Structurally, lysophosphatidylcholine differs from the corresponding diacylphosphatidylcholine by having the entire *sn*-2 acyl chain substituted with a hydrogen atom, and it is thus a unique molecular species of membrane phospholipid in that it exhibits the maximal chain length asymmetry. Recently, it has been shown by high-sensitivity differential scanning calorimetry and Raman spectroscopy that aqueous dispersions of 1-stearoyllysophosphatidylcholine or C(18):C(0)PC can undergo a sharp lamellar to micellar transition at 26.2 °C (Wu et al., 1982). The kinetic study of the micellar → lamellar transition for C(18):C(0)PC suggests that the mechanism of lamellar formation is that of two-dimensional nucleation followed by a growth process (Wu & Huang, 1983). Furthermore, $^{31}P$ NMR studies indicate that the head group motion of C(18):C(0)PC in lamellae is distinctively different from that of diacyl phosphatidylcholine (Wu et al., 1984). However, the packing of lamellar C(18):C(0)PC has been *assumed* in all these biophysical and biochemical studies to adopt a fully interdigitated model on the basis of the highly asymmetrical structure of the C(18):C(0)PC molecule. In this paper, we put forward the first X-ray diffraction evidence to demonstrate that hydrated C(18):C(0)PC forms bilayers at temperatures below the order/disorder transition ($T_m$ = 26.2 °C) and that each C(18):C(0)PC molecule in the bilayer exhibits packing characteristics that are in complete accord with the fully interdigitated model in which the long C(18) acyl chain extends across the entire hydrocarbon width of the bilayer.

## Materials and Methods

1-Stearoyllysophosphatidylcholine [C(18):C(0)PC] was purchased from Avanti Polar Lipids Inc., Birmingham, AL. Prior to sample preparation, the lipid was stored at −70 °C in a desiccator. Lipid suspensions were prepared by adding a known weight of aqueous KCl solution (0.1 M) containing 5 mM Tris buffer, pH 7.4, to an appropriate amount of a preweighed sample of C(18):C(0)PC. In case that an excess amount of $H_2O$ was present, the lipid–$H_2O$ sample was first warmed to 30 °C to form a clear solution and was vortexed for several minutes at this elevated temperature. Subsequently, it was allowed to cool at 4 °C and then concentrated by centrifugation at 6000*g* for 10 min. The centrifuged sample of known concentration was micropipetted into a thin-wall X-ray capillary tube or a holder with mica windows. The tube was incubated at 4 °C for a prolonged period prior to X-ray diffraction studies of the sample at a desired temperature.

The method for X-ray diffraction was described previously (Hui et al., 1984). Briefly, the lipid sample of a given weight percent was mounted in a temperature-controlled cell. The X-ray diffraction patterns were recorded on X-ray films by a Franks-type X-ray camera with slit focusing and a Jarrell-Ash X-ray generator. The optical density of the X-ray diffraction pattern was densitometered with a Joyce-Loebl Mark III microdensitometer.

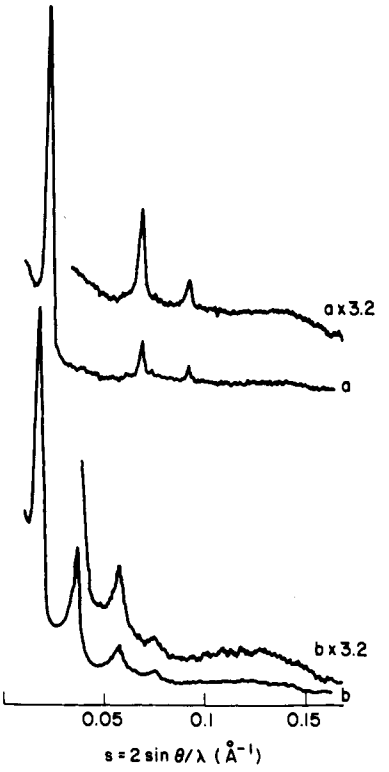


FIGURE 1: Small-angle X-ray diffraction intensities of C(18):C(0)PC at (a) 20 °C, $C$ = 70% (by weight) and (b) 10 °C, 65% (by weight).

## Results

The small-angle X-ray diffraction pattern of hydrated C(18):C(0)PC at temperatures below the order/disorder transition temperature (26.2 °C) shows a series of reflections (Figure 1). The reciprocal spacings of the reflection peaks are in the ratios of 1:2:3..., indicating a stacked lamellar packing. The lamellar repeat spacing varies with hydration as well as with temperature. Moreover, the relative intensity of the peaks depends on the lamellar repeat spacing (Figure 1). A plot of the repeat spacing as a function of hydration at various temperatures is presented in Figure 2. Below the lipid concentration of 58% by weight, the lamellar repeat spacings stay more or less constant at 62 Å. However, if the lipid in excess water was preincubated at 4 °C for less than 48 h, the predominant small-angle diffraction pattern had a larger repeat spacing of 66 Å. At higher lipid concentration, the repeat spacing decreases linearly to 41 Å. Since the precise

[1] Abbreviations: C(18):C(0)PC, 1-stearoyllysophosphatidylcholine; C($x$):C($y$)PC, saturated mixed-chain phosphatidylcholine having $x$ carbons in the *sn*-1 acyl chain and $y$ carbons in the *sn*-2 acyl chain; diC($x$)PC, saturated symmetric phosphatidylcholine having identical $x$ numbers of carbons in each of its *sn*-1 and *sn*-2 acyl chains; $T_m$, main order/disorder transition temperature; Tris, tris(hydroxymethyl)aminomethane.

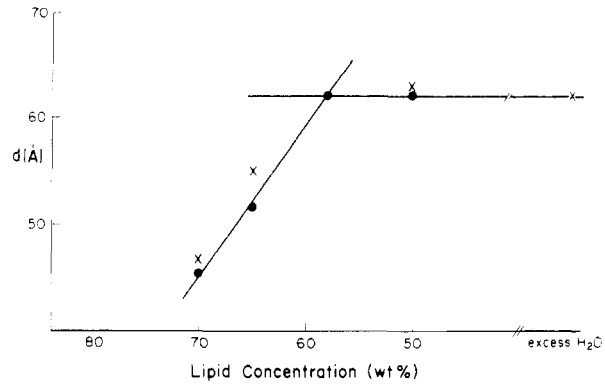


FIGURE 2: Lamellar repeat spacings of C(18):C(0)PC bilayers as a function of lipid concentration at 20 (○) and 10 °C (×).

intrinsic hydration of this lysophosphatidylcholine is unknown, the degree of hydration is taken as the amount of water added to make up the samples.

Assuming that the bilayer thickness remains constant during the hydration process, the bilayer thickness $d_l$ and the average area per molecule at the lipid/water interface $S$ can be obtained from the swelling curve with the formulas (Luzzati, 1968):

$$d_l = d/[1 + \bar{v}_l(1 - C)/(\bar{v}_w C)]$$

$$S = [2M\bar{v}_l/(d_l N)] \times 10^{-24}$$

where $C$ is the concentration (wt %) of the lipid at saturated hydration, $\bar{v}_l$ is the partial specific volume (mL/g) of the lipid, $\bar{v}_w$ is the partial specific volume of water, $d$ is the lamellar repeat spacing (Å) at saturated hydration, $M$ is the molecular weight of the lipid (523.7 g/mol), and $N$ the Avogadro number. The partial specific volume for C(18):C(0)PC has not been reported in the literature. However, the C(18) acyl chain is known as one of the most abundant components of acyl chains at the *sn*-1 position in egg phosphatidylcholine, and an average value of partial specific volume for egg lysophosphatidylcholine is 0.925 mL/g (Steele et al., 1978); hence, we assign the value of 0.925 mL/g as an apparent partial specific volume for C(18):C(0)PC. With this value, a bilayer thickness of 36 Å and an average area per C(18):C(0)PC at the lipid/water interface of 45.5 Å$^2$ can be calculated. It should be pointed out that the partial specific volume ($\bar{v}_l$) of phospholipids in the lipid–$H_2O$ system is relatively insensitive to the physical state of the system. The largest change in $\bar{v}_l$ for synthetic phosphatidylcholines occurs at the gel → liquid-crystalline phase transition, and the overall relative change in $\bar{v}_l$ across the phase transition temperature is merely 3.7% for dipalmitoylphosphatidylcholine dispersions (Nagel & Wilkinson, 1978). Though the exact value of $d_l$ depends on the partial specific volume of lipid in the lipid–$H_2O$ system under study, the effect is rather small: reducing $\bar{v}_l$ by 3.7% from 0.925 mL/g increases the bilayer thickness by approximately 0.5 Å, which is certainly within the experimental error of our X-ray diffraction measurements. Consequently, the value of 0.925 mL/g as the partial specific volume for C(18):C(0)PC used in the bilayer thickness calculation is a reasonable choice.

In order to obtain more information about the detailed structure of the C(18):C(0)PC bilayer, the diffracted intensities of a series of X-ray diffraction patterns from C(18):C(0)PC samples at various stages of swelling were measured. The absolute values of diffraction amplitudes of the $h$th order reflections, normalized by the factor $h$ (McIntosh, 1978), are plotted in Figure 3 as a function of their reciprocal spacing.

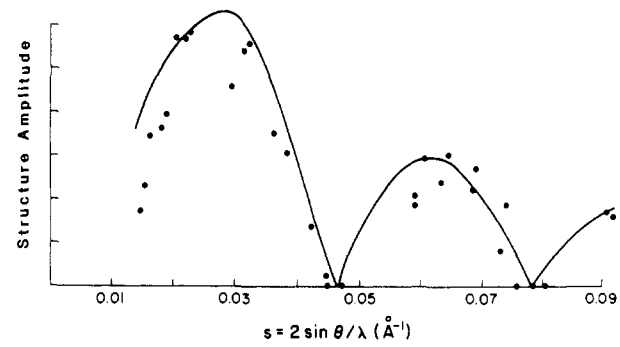


FIGURE 3: Absolute values of diffraction amplitude at various spacings measured from C(18):C(0)PC samples at different degrees of swelling. The continuous curve is calculated from an inverse Fourier transformation from the electron-density profile on the basis of the data set given in Figure 1a and the phase combination of ($\pi$, 0, $\pi$).

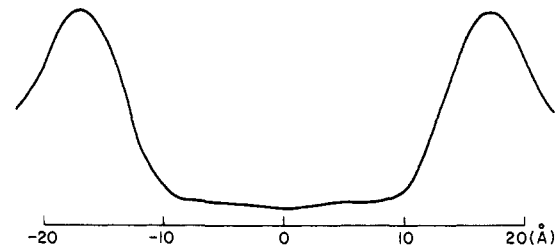


FIGURE 4: Electron-density profile derived from the intensity data set given in Figure 1a and the phase combination of ($\pi$, 0, $\pi$). (See text for the choice of phase combination.)

The enveloping function represents the absolute value of the structure factor, assuming that the centrosymmetric structure of the bilayer remains unchanged during the swelling process. These absolute amplitudes fall in three distinct groups. Since lysophospholipid bilayers are assumed to be centrosymmetric, the phase can only be either $\pi$ or 0. The points of zero intensities correspond to the positions of possible phase changes. The three groups of amplitudes would have $2^3 = 8$ possible phase combinations. We have tried all different phase combinations and derived the electron-density profiles by the Fourier methods using two sets of diffraction amplitudes. Only those phase combinations with alternating phases give similar inverse Fourier transforms between the two data sets. This narrows down the phase choice to be either ($\pi$, 0, $\pi$) or (0, $\pi$, 0) for the three regions of the transform. These two choices of phase combinations yield electron-density profiles of opposite polarity. Following the convention of bilayer structure calculation of McIntosh (1978), the ($\pi$, 0, $\pi$) phase combination for the structural factor amplitudes for C(18):C(0)PC lamellae was chosen to calculate the electron-density profile.

An electron-density profile for C(18):C(0)PC is shown in Figure 4 of the diffraction data with a 45.5-Å repeat spacing, which has the highest resolution of 11 Å. This profile is characterized by two outermost high electron density peaks centered at ±17.5 Å and a relatively uniform low electron density region between the peaks. The separation of 35 Å between the high electron density peaks is observed for C(18):C(0)PC at all stages of the swelling. With the conventional interpretation of bilayer electron density profiles, the high electron density peaks can be assigned to the location of the phosphate moiety of lipid head groups, and the low-density region corresponds to the lipid hydrocarbon chains of the bilayer interior. Consequently, the distance between the peaks in the one-dimensional electron-density profile is a measure of the bilayer thickness. It should be noted that the bilayer thickness of 35 Å determined from the electron-density profile is in excellent agreement with that of 36 Å obtained by the

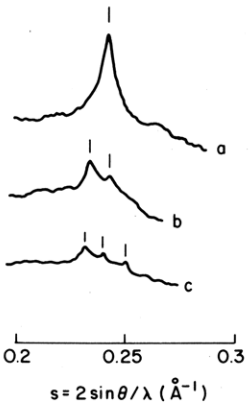


FIGURE 5: Wide-angle X-ray diffraction patterns of C(18):C(0)PC recorded at (a) 20 °C, $C$ = 70% (by weight), (b) 10 °C, $C$ = 65%, and (c) 20 °C, $C$ = 58%.

saturation hydration method for C(18):C(0)PC lamellae.

The wide-angle diffraction of C(18):C(0)PC at low hydration with a 45.5-Å lamellar repeat spacing shows a sharp band centered at 4.11 Å (Figure 5a). In more hydrated samples with longer lamellar repeat spacings, multiple overlapping reflections appear. These multiple reflections (4.26 and 4.11 Å in Figure 5b and 4.31, 4.16, and 4.00 Å in Figure 5c) become less distinguishable at higher water content, as indicated in Figure 5b,c.

## Discussion

Largely on the basis of X-ray crystal structures of phosphatidylethanolamine and phosphatidylcholine (Hitchcock et al., 1974; Pearson & Pascher, 1979), it is now well recognized that in the gel-state bilayer of pure symmetric phospholipids the *sn*-2 acyl chain of phospholipid molecules lies initially parallel to the bilayer surface and the chain then bends abruptly at the C(2) atom so that the rest of the *sn*-2 chain runs parallel to the all-trans *sn*-1 chain. An important structural feature resulting from the *sn*-2 chain bend is that the two terminal methyl groups of the two acyl chains in the gel-state bilayer are not in register, being separated by a distance of approximately 1.8 Å or 1.5 C–C bond length (Seelig and Seelig, 1980). Taking the chain bend into consideration, the absolute difference in chain length between the *sn*-1 and *sn*-2 chains for a mixed-chain saturated phospholipid in the gel-state bilayer can be quantitatively defined by a parameter, $\Delta C$, which is given by the equation $\Delta C = |n_1 - n_2 + 1.5|$, where $n_1$ and $n_2$ are the number of carbon atoms in the *sn*-1 and *sn*-2 acyl chains, respectively (Mason et al., 1981). After it is divided by the chain length of the longer of the two acyl chains (CL), the normalized value of the chain-length difference $\Delta C$/CL can be employed to map out the specific region in which a particular type of chain interdigitation is expected (Mason et al., 1981).

It is obvious that phosphatidylcholines such as C(14):C(16)PC and C(16):C(18)PC with $\Delta C$ = 0.5 carbon–carbon bond length (or $\Delta C$/CL $\simeq$ 0.035) will adopt a noninterdigitated packing arrangement in the gel-state lamella. In this packing mode, the chain methyl termini are accommodated in the geometric center of the bilayer (Figure 6a).

Phosphatidylcholine molecules with their $\Delta C$ values larger than 0.5 but smaller than 6 carbon–carbon bond length ($6 > \Delta C > 0.5$) will, in the gel-state bilayer, adopt a partially interdigitated packing arrangement, in which the longer chain of the lipid on one side of the bilayer will pack end to end with the shorter chain of another lipid molecule in the opposing bilayer leaflet (Figure 6b). Mixed-chain phospholipids such

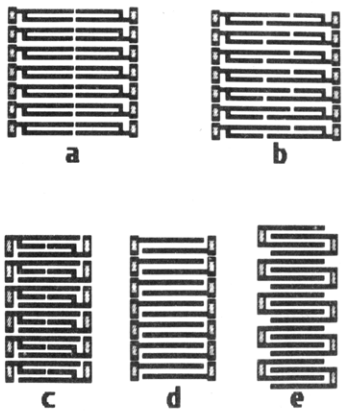


FIGURE 6: Interdigitated and noninterdigitated bilayer models showing schematically the various chain-packing geometries. Dashed rectangular boxes represent the phosphatidylcholine head group, and the filled bars represent the fatty acyl chain. A sharp bend is incorporated in the *sn*-2 acyl chain.

as C(16):C(14)PC, C(18):C(16)PC, and C(18):C(14)PC serve as examples for the partially interdigitated lipid species (Hui et al., 1984; Serrallach et al., 1984).

As the chain length difference increases to the optimal value such that it is about half of the longer chain length ($0.6 > \Delta C$/CL $> 0.4$), the lamellar lipids exhibit a mixed interdigitated packing arrangement (Hui et al., 1984; McIntosh et al., 1984). Examples of this mixed interdigitation can be drawn from C(18):C(10)PC ($\Delta C$/CL = 0.56) and C(18):C(12)PC ($\Delta C$/CL = 0.44). In this case, the methyl terminus of the shorter chain is packed end to end, at the bilayer center, with the methyl terminus of the shorter chain from another lipid molecule in the opposing bilayer leaflet, while the longer chain from the two leaflets spans the entire hydrocarbon width of the bilayer (Figure 6c). The mixed interdigitated gel bilayer is thus characterized by having the area per molecule at the lipid/water interface encompass three hydrocarbon chains, in contrast to the two hydrocarbon chains per lipid head group for phosphatidylcholines in the noninterdigitated and partially interdigitated bilayers.

As the difference between the length of the two acyl chains increases to the maximal limit such that the ratio of $\Delta C$/Cl is approximately unity as exampled by C(18):C(2)PC ($\Delta C$/CL = 1.03), a third type of interdigitated gel-state bilayer becomes favorable (Huang et al., 1984). In this fully interdigitated form, each long acyl chain spans the entire hydrocarbon width of the bilayer and interacts laterally with the long acyl chain of lipid molecules from the opposing lamellar leaflet (Figure 8d). The average area per lipid molecule at the lipid/water interface is about twice the cross-sectional area of an all-trans acyl chain. Recently, Jain et al. (1985) has involved this full interdigitation model to explain that X-ray diffraction data obtained for gel-state lamellae of a C(18):C(0)PC analogue, *n*-octadecylphosphocholine. In fact, the full interdigitation model has long been suggested by Ranck et al. (1977, 1982a,b) for the bilayer of symmetric diacyl phospholipids such as dipalmitoylphosphatidylglycerol under special circumstances (Figure 8e).

On the basis of the highly asymmetric structure of C(18):C(0)PC ($\Delta C$/CL = 1.15), it has been assumed by Wu et al. (1982) that the C(18):C(0)PC bilayer has a fully interdigitated packing arrangement (Figure 8d). The present X-ray diffraction data indeed confirm this. First, the bilayer thickness of 35–36 Å for C(18):C(0)PC, as determined from the saturation hydration method and electron-density profile, is significantly smaller than that of 52 Å determined for

diC(18)PC bilayers (Chapman et al., 1967). One possible explanation for the shorter lamellar thickness could be attributed to the chain tilt. In order to shorten the bilayer thickness from 52 to 35 Å, the tilting angle with respect to the bilayer normal would have to be 47.7°. Bilayers with such a large chain tilt would exhibit in the wide-angle region an asymmetric X-ray diffraction envelope (Tardieu et al., 1973). Since the wide-angle band is sharp and symmetrical (Figure 5a), the smaller bilayer thickness cannot represent a noninterdigitated lamellar structure with pronounced hydrocarbon chain tilt. The observed bilayer thickness (35–36 Å) is, however, consistent with the packing geometry of fully interdigitated hydrocarbon chains in an all-trans configuration, because the bilayer thickness for C(18:)C(0)PC is virtually identical with the sum of the full length of stearic acid (27 Å) and the overall thickness of phosphatidylcholine head groups (7.3 Å) in the bilayer (Hauser et al., 1982). Second, the characteristic low electron density trough in the geometric center of the one-dimensional profile for noninterdigitated bilayers is lacking from our electron-density profile (Figure 4). Since the low electron density trough corresponds to the chain terminal methyl groups (McIntosh 1978), the absence of a prominent dip in our electron-density profile may be readily interpreted as arising from the penetration of chain methyl termini across the entire hydrocarbon width of the bilayer to the glycerol backbone region in the opposing lamellar leaflet. This, of course, favors a fully interdigitated bilayer. The absence of a trough in the electron-density profile is not a truncation artifact from our 11-Å resolution data, since diffraction data of similar resolution from noninterdigitated bilayers do show a pronounced trough [not shown, see McIntosh (1978)]. Finally, the average area per C(18):C(0)PC at the lipid/water interface is estimated to be 45.5 Å$^2$, and the cross-sectional area of the acyl chain can be calculated from the wide-angle spacing ($d_{01}$ = 4.11 Å) to be $2d_{01}^2/3^{1/2}$ = 19.5 Å$^2$ (Tardieu et al., 1973). The surface area per C(18):C(0)PC is thus about twice the cross-sectional area of an all-trans acyl chain in the lamellar gel phase. Such a ratio is consistent with the packing model of fully interdigitated bilayers comprised of single-chain phospholipids.

The physical state (crystalline, gel, or liquid crystalline) and the two-dimensional packing mode of C(18):C(0)PC acyl chains in the fully interdigitated bilayer can be estimated from the X-ray diffraction pattern in the wide-angle region. At low hydration, the wide-angle pattern contains a sharp, symmetric reflection at $d_{01}$ = 4.11 Å (Figure 5a), indicating that the C(18) hydrocarbon chains are packed in a hexagonal lattice in the plane of the bilayer, with interchain distance of a = $(2/3)^{1/2}d_{01}$ = 4.7 Å. At higher hydration, the 4.11-Å reflection splits into multiple peaks positioned at both longer and shorter spacings (Figure 5c). The display of relatively sharp peaks at long spacings by C(18):C(0)PC in the wide-angle regions is different from the symmetrical and broad 4.6-Å reflection characteristic of phospholipid acyl chains packed in the disordered lamellar liquid-crystalline phase (Luzzati, 1968). Furthermore, the overlapping features of a series of bands (the stronger bands at 4.31, 4.16, and 4.00 Å are marked in Figure 5c) does not match with either an asymmetric envelope consisting of a peak and a shoulder, characteristic of the degenerate 4.2-Å reflection resulting from chain tilt (Hui, 1976; Janiak et al., 1976; Tardieu et al., 1973), or the discrete symmetrical double peaks characteristic of a highly ordered two-dimensional orthorhombic hydrocarbon chain packing (Hoerr & Paulicka, 1968; Lutton, 1950). The hydration-dependent X-ray diffraction patterns observed in Figure 5 imply that with increasing hydration the two-dimensional packing lattice of acyl chains in the C(18):C(0)PC assembly undergoes a transformation from one with high symmetry into one with lower symmetry. Because not all of the wide-angle reflections are clearly resolvable, no attempt was made to identify them. It should be noted, however, that the wide-angle multiple reflections remain relatively sharp at high water content, indicating that the intrachain disorder has not been increased appreciably from lattice-transformation phenomena with increasing hydration; hence, the C(18):C(0)PC bilayer remains in the gel state at higher water content.

Figure 6 summarizes various bilayer models depicting some of the possible acyl chain packing geometries for fully hydrated phosphatidylcholine molecules in the gel state. Model a is commonly recognized in bilayers with no chain interdigitation. This is probably the most common one for biological membrane lipids, for example, 1-palmitoyl-2-oleoyl-*sn*-glycero-3-phosphocholine, but is not necessarily the most energetically favorable configuration. This model, however, may be the only possible gel-state packing from some synthetic mixed-chain phospholipids. For pure saturated phospholipids with identical acyl chain composition, the noninterdigitated form may represent only a metastable state. Model b is designated as the partially interdigitated bilayer, which is configurationally a stable state for phospholipids with a small value of $\Delta C$. The interdigitation of the acyl chains in this form can impose severe restrictions on the rotational motion of the molecule as a whole in the bilayer, especially at low temperatures, giving rise to a characteristic herringbone orientation of hydrocarbon chains in the two-dimensional plane of the bilayer. Such an ordering of hydrocarbon chains is a common feature observed for phospholipids in the subgel or $L_c$ phase (Chen et al., 1980; Füldner, 1981; Ruocco & Shipley, 1982). Models c–e are special cases of interdigitated bilayers preferred by various phospholipids under a wide range of conditions. It is noteworthy to mention that a highly asymmetric molecular species of sphingomyelin, *erythro-N*-lignoceroylsphingosylphosphocholine, with a value of $\Delta C$/CL approximately equal to 0.5, is observed to form the mixed interdigitated bilayer (model c) in excess water at physiological temperatures (Levin et al., 1985). In this paper, we provide X-ray diffraction evidence to show that hydrated C(18):C(0)PC forms fully interdititated bilayers (model d). Judging from the molecular structure of the platelet-activating factor (1-*O*-octadecyl-2-acetoyl-*sn*-glycero-3-phosphocholine), one would predict that in excess water this interesting biological lipid with a $\Delta C$/CL value of about unity will most likely form fully interdigitated lamellae at temperatures below $T_m$, similar to the structurally closely related molecular species of C(18:)C(0)PC. Work is now under way in our laboratories to characterize the aqueous dispersions of platelet-activating factor.

**Registry No.** C(18):C(0)PC, 5655-17-4.

## REFERENCES

Chapman, D., Williams, R. M., & Ladbrook, B. D. (1967) *Chem. Phys. Lipids 1*, 445–475.

Chen, S. C., Sturtevant, J. M., & Gaffney, B. J. (1980) *Proc. Natl. Acad. Sci. U.S.A. 77*, 5060–5063.

Colbeau, A., Nachbar, J., & Vignois, P. M. (1971) *Biochim. Biophys. Acta 249*, 462–472.

Füldner, H. H. (1981) *Biochemistry 20*, 5707–5710.

Hauser, H., Pascher, I., Pearson, R. H., & Sundell, S. (1981) *Biochim. Biophys. Acta 650*, 21–51.

Hitchcock, P. B., Mason, R., Thomas, K. M., & Shipley, G. G. (1974) *Proc. Natl. Acad. Sci. U.S.A. 71*, 3036–3040.

Hoerr, C. W., & Paulicka, F. R. (1968) *J. Am. Oil Chem. Soc. 45*, 793–797.
Huang, C., Mason, J. T., Stephenson, F. A., & Levin, L. W. (1984) *J. Phys. Chem. 88*, 6454–6458.
Hui, S. W. (1976) *Chem. Phys. Lipids 16*, 9–18.
Hui, S. W., Mason, J. T., & Huang, C. (1984) *Biochemistry 23*, 5570–5577.
Jain, M. K., Crecely, R. W., Hille, J. D. R., deHaas, G. H., & Gruner, S. M. (1985) *Biochim. Biophys. Acta 813*, 68–76.
Janiak, M. J., Small, D. M., & Shipley, G. G. (1976) *Biochemistry 15*, 4575–4580.
Levin, I. W., Thompson, T. E., Barenholz, Y., & Huang, C. (1985) *Biochemistry 24*, 6282–6286.
Lutton, E. S. (1950) *J. Am. Oil Chem. Soc. 27*, 276–281.
Luzzati, V. (1968) in *Biological Membranes* (Chapman, D., Ed.) pp 71–124, Academic Press, New York.
Mason, J. T., Huang, C., & Biltonen, R. L. (1981) *Biochemistry 20*, 6086–6092.
McDaniel, R. V., McIntosh, T. J., & Simon, S. A. (1983) *Biochim. Biophys. Acta 731*, 97–108.
McIntosh, T. J. (1978) *Biochim. Biophys. Acta 513*, 43–58.
McIntosh, T. J., McDaniel, R. V., & Simon, S. A. (1983) *Biochim. Biophys. Acta 731*, 109–114.
McIntosh, T. J., Simon, S. A., Ellington, J. C., & Porter, N. A. (1984) *Biochemistry 23*, 4038–4044.
Nagle, J. F., & Wilkinson, D. A. (1978) *Biophys. J. 23*, 159–175.
Nelson, G. J. (1967) *Biochim. Biophys. Acta 144*, 221–232.
Pearson, R. H., & Pascher, I. (1979) *Nature (London) 281*, 499–501.
Ranck, J. L., & Tocanne, J. F. (1982a) *FEBS Lett. 143*, 171–174.
Ranck, J. L., & Tocanne, J. F. (1982b) *FEBS Lett. 143*, 175–178.
Ranck, J. L., Keira, T., & Luzzati, V. (1977) *Biochim. Biophys. Acta 488*, 432–441.
Ruocco, M. J., & Shipley, G. G. (1982) *Biochim. Biophys. Acta 691*, 309–320.
Ruocco, M. J., Siminovitch, D. J., & Griffin, R. G. (1985) *Biochemistry 24*, 2406–2411.
Seelig, J., & Seelig, A. (1980) *Q. Rev. Biophys. 13*, 19–61.
Serrallach, E. N., de Hass, G. H., & Shipley, G. G. (1984) *Biochemistry 23*, 713–720.
Simon, S. A., & McIntosh, T. J. (1984) *Biochim. Biophys. Acta 733*, 169–172.
Steele, J. C. H., Tanford, C., & Reynolds, J. A. (1978) *Methods Enzymol. 48*, 11–23.
Tardieu, A., Luzzati, V., & Reman, F. C. (1973) *J. Mol. Biol. 75*, 711–733.
Theretz, A., Ranck, J. L., & Tocanne, J. F. (1983) *Biochim. Biophys. Acta 732*, 499–508.
Wu, W., & Huang, C. (1983) *Biochemistry 22*, 5068–5073.
Wu, W., Huang, C., Conley, T. G., Martin, R. B., & Levin, I. W. (1982) *Biochemistry 21*, 5957–5961.
Wu, W., Stephenson, F. A., Mason, J. T., & Haung, C. (1984) *Lipids 19*, 68–71.

# Predicted Membrane Topology of the Coronavirus Protein E1

Peter J. M. Rottier,[‡] Gjalt W. Welling,[§] Sytske Welling-Wester,[§] Hubert G. M. Niesters,[‡] Johannes A. Lenstra,[‡] and Bernard A. M. Van der Zeijst*,[‡]

*Institute of Virology, Veterinary Faculty, State University, Yalelaan 1, 3508 TD Utrecht, The Netherlands, and Laboratory of Medical Microbiology, State University, Oostersingel 59, 9713 EZ Groningen, The Netherlands*

*Received August 16, 1985*

ABSTRACT: The structure of the envelope protein E1 of two coronaviruses, mouse hepatitis virus strain A59 and infectious bronchitis virus, was analyzed by applying several theoretical methods to their amino acid sequence. The results of these analyses combined with earlier data on the orientation and protease sensitivity of E1 assembled in microsomal membranes lead to a topological model. According to this model, the protein is anchored in the lipid bilayer by three successive membrane-spanning helices present in its N-terminal half whereas the C-terminal part is thought to be associated with the membrane surface; these interactions with the membrane protect almost the complete polypeptide against protease digestion. In addition, it is predicted that the insertion of E1 into the membrane occurs by the recognition of the internal transmembrane region(s) as a signal sequence.

Proteins synthesized in eukaryotic cells have divergent destinations. Either they stay in the cytoplasm, or they are transported to organelles, to the plasma membrane, or out of the cell. Little is known about the determinants that direct a protein to its particular destination. It is generally assumed that such determinants reside in the protein's specific structure. Recently, we have presented the E1 glycoprotein of coronavirus mouse hepatitis virus A59 (MHV-A59)[1] as a model intracellular protein, the study of which might give insight into the targeting principles of such proteins (Rottier et al., 1984, 1985; Armstrong et al., 1984).

In contrast to most other enveloped RNA viruses, coronaviruses bud into the endoplasmic reticulum (ER) (Holmes & Behnke, 1981; Niemann et al., 1982; Tooze et al., 1984). This particular budding site is determined by the envelope glyco-

[‡] Institute of Virology.
[§] Laboratory of Medical Microbiology.

[1] Abbreviations: ER, endoplasmic reticulum; IBV, infectious bronchitis virus; MHV-A59, mouse hepatitus virus strain A59; SRP, signal-recognition particle.

0006-2960/86/0425-1335$01.50/0 